Article

PSI-mediated vacuolar sorting is not disrupted in Arabidopsis *leb-2* mutant

Tatiana Cardoso [1], Miguel Sampaio [1,2], João Neves[1], Sofia Oliveira[1], Inês Moura[1], Ana Séneca [1,2], José Pissarra [1,2], Susana Pereira [1,2] and Cláudia Pereira [1,2,*]

[1] Faculdade de Ciências, Universidade do Porto, Rua do Campo Alegre, s/n_, 4169-007 Porto, Portugal; tatiffcardoso_902@hotmail.com (T.C.); up201503801@edu.fc.up.pt (M.S.); up201704802@edu.fc.up.pt (J.N.); up201704356@edu.fc.up.pt (S.O.); up201805266@edu.fc.up.pt (I.M.); aseneca@fc.up.pt (A.S.); jpissarr@fc.up.pt (J.P.); mspereir@fc.up.pt (S.P.); cpereira@fc.up.pt (C.P.)

[2] GreenUPorto-Sustainable Agrifood Production Research Centre and Inov4Agro - Institute for Innovation, Training and Sustainability of Agrifood Production, Rua do Campo Alegre s/n, 4169-007 Porto, Portugal

* Correspondence: cpereira@fc.up.pt

Abstract: The endomembrane system in plant cells enables the cell to manage and coordinate a variety of membranous compartments so that they and their contents arrive at the right location. The secretory pathway takes part in this complex network and has its gateway at the Endoplasmic Reticulum. Therefore, alterations at the Endoplasmic reticulum level could condition how protein trafficking takes place or, at least, influence how such cargo leaves this organelle. With this work, we intended to assess how abnormalities at the Endoplasmic Reticulum would interfere with protein sorting and trafficking. Thus, we used a novel Arabidopsis mutant - *leb-2 GFP-h* -, presenting ER morphology alterations. Our results show that alterations in the *leb-2 GFP-h* mutant did not disrupt PSI A/B–mCherry transport to the vacuole but influences the expression of endogenous aspartic proteinases. Furthermore, the study of key-endomembrane genes expression revealed an upregulation of the SNAREs AtVAMP722 and AtVAMP723. As a whole, the *leb-2* mutant seems not to interfere with vacuolar routes but may be implicated in secretion events.

Keywords: Arabidopsis; ER-bodies; aspartic proteinases; Plant Specific Insert; Vacuolar sorting; Endomembranes

1. Introduction

The endomembrane trafficking system of eukaryotic cells is critical for essential cellular processes, such as maintaining cellular homeostasis and proliferation, as well as multicellular organism-specific requirements [1,2]. This network of membrane compartments responsible for cargo molecules delivery is especially complex and well-coordinated in plant cells, occurring along several compartmentalized organelles: the Endoplasmic Reticulum (ER), the Golgi, the Trans-Golgi Network (TGN), the Pre-vacuolar Compartment (PVC), the Vacuole, secretory vesicles, and endosomes [3–6]. In plants, the secretory pathway begins in the ER. This flexible and multifunctional organelle contacts with several other key structures in the cell, including the plasma membrane (PM), the Golgi, endosomes, lysosomes, mitochondria, and peroxisomes, in a three-dimensional network of continuous tubules and cisterns. Thereby, this organelle communicates with numerous membrane compartments along both the secretory and endocytic pathways [7–9]. Differently from what is observed in mammalian cells and yeasts, in plants the ER is restricted to a small space between the plasma membrane (PM) and the tonoplast of the vacuole in the cytoplasm, while maintaining its extensive distribution and movement in the cell [10,11]. Some organisms may even produce distinctive ER-derived structures, like the ER bodies, which are spindle-shaped storage

 doi:10.20944/preprints202304.0023.v1

spaces for the build-up of large amounts of glucosidase (PYK10), possibly involved in plant defence mechanisms and are present in Brassicaceae plants and some related species [12,13]. In addition, ER bodies may function as intermediates in trafficking routes to the vacuole in response to ER stress [14], underscoring the adaptability of this organelle in plant cells.

Conventionally, proteins trafficking through the secretory pathway are led from the ER to the Golgi apparatus and then reach their final location, which may be the vacuole, other compartments, or the PM [15,16]. Since plant cells have two distinct types of vacuoles (protein storage vacuoles (PSVs), and lytic vacuoles (LVs)) and both may be found within the same cell [17,18], it is crucial to comprehend the mechanisms and regulation governing vacuolar trafficking, as vacuoles are essential for maintaining the homeostasis of plant cells. Our laboratory has been especially interested in cardosin A and cardosin B, two well-characterized aspartic proteinases (APs) found in *Cynara cardunculus* [19,20]. Although highly similar in protein sequence, these enzymes are stored in different cell compartments as plants develop [20,21]. It has been evidenced that cardosin A differentiates its accumulation in PSVs or LVs, according to the developmental stage and particular cellular requirements [21–24], whereas cardosin B is found extracellularly [20]. Yet, when expressed in Arabidopsis thaliana and Nicotiana tabacum, both cardosins A and B demonstrated the same localization patterns, being found in LVs [25–27]. Such features make cardosins puzzling and intriguing study objects, offering solid evidence for their usefulness as reporters in studying vacuolar trafficking and vacuolar sorting determinants (VSDs) in plants.

Plant-specific inserts (PSIs) are unique protein domains of about 100 amino acids [28,29] found in both cardosin A and B. Since this domain exhibits multiple functions, when isolated and in vitro, including acting as a detergent, mediating lipid membrane interactions, exhibiting putative antimicrobial activity, inducing membrane permeabilization, along with membrane modulation, it is frequently referred to as "an enzyme within an enzyme" [30–34]. Even if its roles in cells remain to be fully established, the PSI has been linked to APs' vacuolar targeting [25,30,34]. With the emergence of novel unconventional routes for vacuolar sorting, with proteins being directly sorted to the LV from the ER [26,35–38], it is indispensable to understand where the PSI fits in the complex network of vacuolar protein trafficking. Although the AP can be directed to the vacuole by both the cardosin A PSI (PSI A) and the cardosin B PSI (PSI B), the ways in which they do so differ greatly. In contrast to PSI A-mediated sorting, which is COPII-independent, PSI B-mediated sorting involves transport from the ER to the Golgi, in a COPII-dependent manner [39]. Besides, little is known about the processes governing this sorting, despite the fact that PSIs are regarded vacuolar sorting determinants given their capacity to mediate trafficking to the vacuole.

To better understand the processes involved in PSI-mediated sorting, and since the ER appears to be a key checkpoint in these routes, we posed the question of whether abnormalities at the ER level affect protein sorting. Thus, we sought and chose an *Arabidopsis thaliana line* with gene mutation causing changes in ER morphology, resorting to the Nottingham Arabidopsis Stock Center (NASC) database, and then we assessed the expression and localization of the PSI domain in such mutants. A codon mutation in the *leb-2 GFP-h* mutant (CCT to TCT) results in a P41S mutation in the PYK10/BGLU23 protein, which elongates ER bodies, thus affecting the route to the PSV. Along with the localization assays performed in this mutant, an ultrastructural characterization was done as well as an evaluation of the expression of the PSIs and other genes involved in the various routes of the endomembrane trafficking system to fully understand the repercussions of the mutations in these plants. Ultimately, we expected to provide deeper knowledge on the interactions taking place among the different organelles of the endomembrane system and how unconventional PSI trafficking and sorting occur within plant cells, along with a rich characterization of the *leb-2 GFP-h* mutant.

Preprints (www.preprints.org) | NOT PEER-REVIEWED | Posted: 3 April 2023 doi:10.20944/preprints202304.0023.v1

2. Results

2.1. Developmental assays of leb-2 GFP-h

The *leb-2 GFP-h* Arabidopsis mutant (Figure 1-A) is not characterized yet, even though a similar phenotype as *leb-1* mutant is expected [40]. Given this, and before starting the expression assays, it was decided to perform a developmental assay to compare several stages of the chronological progression of the plants' growth were evaluated compare its developmental stages of the mutant with the ones from wild type plants. Developmental differences between this line and the WT line are obvious, particularly concerning the size of plants, with *leb-2 GFP-h* presenting a much smaller size (Figure 1-B). As it may be observed in Figure 1-C, until the appearance of the three rosette leaves, both lines reached the selected developmental stages at a similar rate. However, after the next stage evaluated (four rosette leaves), the *leb-2 GFP-h* mutated line presented a delay in development, relative to the WT line, presenting the first siliques well beyond the 140 days after the seeds were sown.

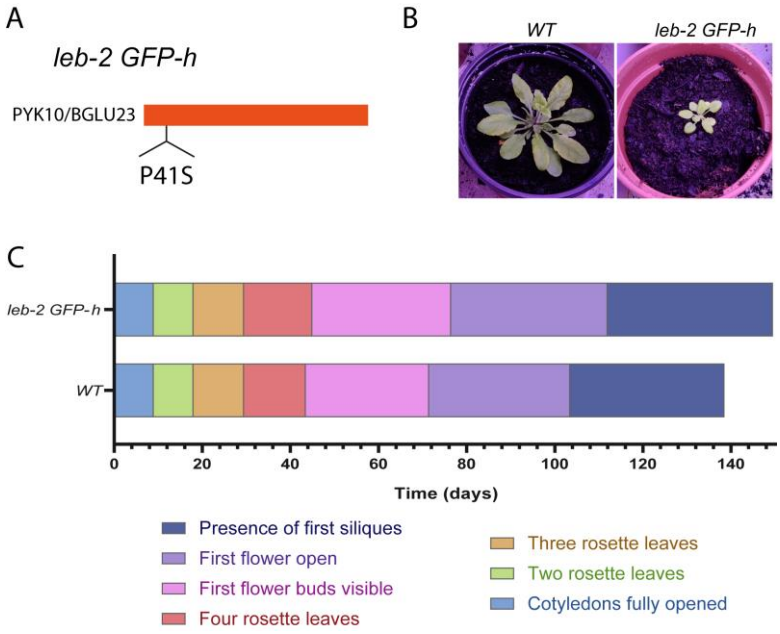

Figure 1 – Developmental stages of the *leb-2 GFP-h* mutated line compared to wild type. (A) Schematization of the *leb-2 GFP-h* mutation in the PYK10/BGLU23 protein. (B) *Arabidopsis thaliana* plants size comparison before appearance of the floral tubes. (C) Chronological progression, in days, of the main growth stages of *A. thaliana* mutated and wild-type lines.

2.2. Microscopic characterization of the ER-defective plants

To further characterize the endomembrane system of the mutated lines, the ultrastructure of the cells from cotyledon leaves was assessed through TEM, allowing a deeper knowledge on the effects of these mutation. Our observations were specially focused on the ER, its associated vesicles, and the Golgi, as these are the most important features in terms of protein sorting, for detection of subtle phenotypes in these organelles. The wild-type line was used as the control and represents the normal organization of the cell, showing organized chloroplasts, some vesicles present in the cytoplasm and normal ER tubules (Figure 2-B-a and b).

Preprints (www.preprints.org) | NOT PEER-REVIEWED | Posted: 3 April 2023 doi:10.20944/preprints202304.0023.v1

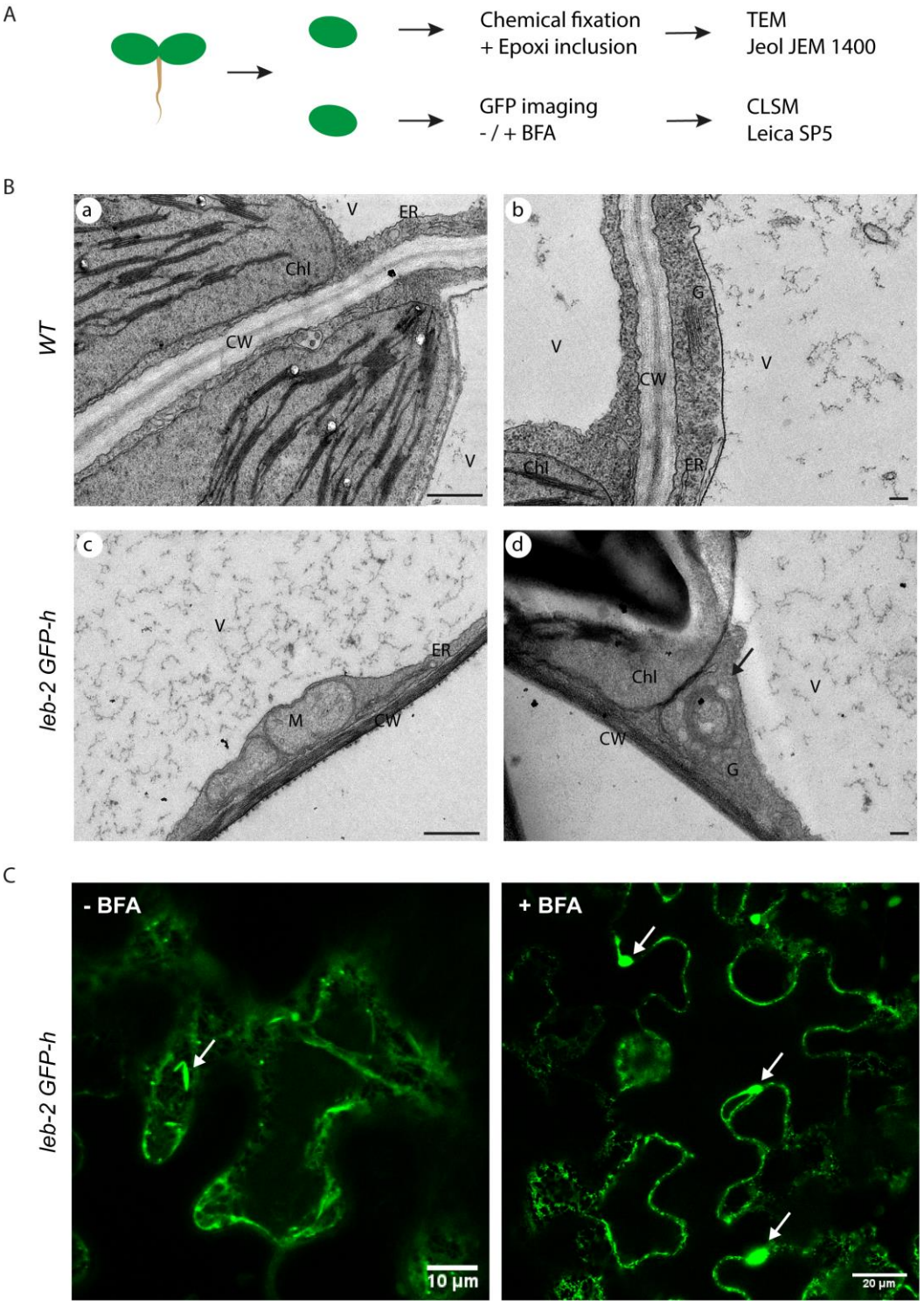

Figure 2 – Ultrastructural and subcellular images from the cotyledon leaves of *leb-2 GFP-h* mutated line. (A) Schematic representation of the workflow for transmission electron microscopy (TEM) and confocal laser scanning microscopy (CLSM). (B) Electron microscopy micrographs of sections of Arabidopsis cotyledon leaves of wild-type (a, b) and *leb-2 GFP-h* lines (c, d). (C) Expression of the GFP-HDEL marker in the epidermis of cotyledon leaves of *leb-2 GFP-h* line seedlings in control conditions (-BFA) and with Brefeldin A (+BFA).

Generally, normal chloroplast shape and thylakoid formation, with the proper thylakoid ultrastructure organization in grana stacks and stroma lamellae were observed. Moreover, the cell's cytoplasm was rich in ribosomes and/or polyribosomes (Figure 2-B-a

 doi:10.20944/preprints202304.0023.v1

and b). Finally, in the *leb-2 GFP-h* mutated line, huge well-defined starch granules were found present in the chloroplasts of the leaf tissues (Figure 2-B-d), indicating some degree of stress. One intriguing feature of this line was the enlarged cisternae of the Golgi apparatus (Figure 2-B-d, black arrow) and numerous vesicles were observed in the cytoplasm in the vicinity of the ER and Golgi. In the analysed tissue, the ER was found to have abnormal morphology, as it appeared to be enlarged in the extremities (Figure 2-B-c). In this mutant, thylakoid membranes appeared loosely packed into grana and it possessed more plastoglobuli (Figure 2-B-d). No ER-bodies were detected in the samples analysed.

Resorting to the expression of the GFP-HDEL present in the *leb-2* mutant, it was also possible to image the ER network using confocal laser scanning microscopy (Figure 2-C). The ER network is clearly visible, along with its tubules and cisternae and some ER-bodies are also detected in the cell cytoplasm (Figure 2-C -BFA, arrow). Then, we assessed if this morphology would be further affected by Brefeldin A (BFA), which is a commonly used fungal macrocyclic lactone that inhibits vacuolar protein transport and secretion in plant cells, resulting in the formation of ER-Golgi hybrid compartments [41]. In the mutant background, when applying BFA, the ER-bodies are no longer visible, and fluorescence aggregates, probably BFA bodies, are visible in the cytoplasm (Figure 2-C +BFA, arrows).

2.3. SP-PSIA/B–mCherry transient expression in the mutated plants

Cardosins' PSIs – PSI A and PSI B – are vacuolar sorting domains, mediating different routes. PSI B mediates a conventional ER-Golgi route, while cardosin A PSI has the ability to follow a Golgi-independent route to the vacuole. However, the nature and the intervenients in such route are not known. To assess whether ER-bodies may participate in the process, we expressed PSI A and PSI B in the *leb-2* mutant background to assess its localization. As before, several images, from different experiments, were captured and analyzed and the most representative are displayed (Figure 3). It is evident by the images shown in Figure 3 that both PSIs are mainly found in the vacuolar compartments both in the WT line and in the *leb-2 GFP-h* line (Figure 3-B, C and D). In the mutant, we may also observe that no co-localization of PSI A/B-mCherry and GFP-HDEL markers was detected (Figure 3-C and D), indicating that at the time of imaging all the protein was already in the vacuole.

Preprints (www.preprints.org) | NOT PEER-REVIEWED | Posted: 3 April 2023 doi:10.20944/preprints202304.0023.v1

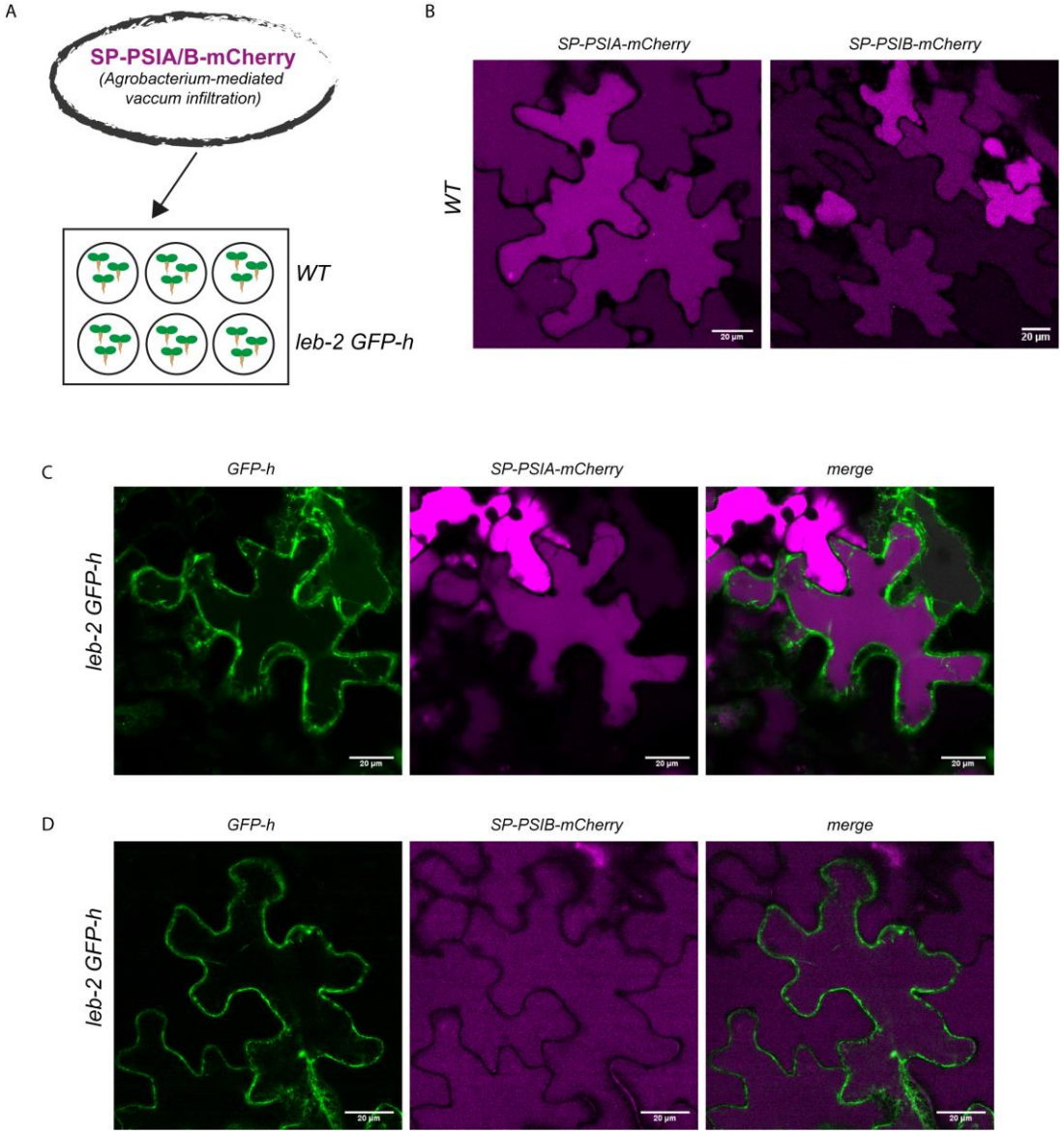

Figure 3 – Subcellular localization of SP-PSIA/B-mCherry in cotyledon leaves of wild-type and *leb-2 GFP-h* seedlings. (A) Workflow of vacuum infiltration setting for transient transformation of Arabidopsis wild-type and *leb-2 GFP-h* seedlings. (B) Expression of PSI A/B-mCherry in wild-type cotyledon leaves. (C) Expression of PSI A-mCherry in *leb-2 GFP-h* cotyledon leaves. (D) Expression of PSI B-mCherry in *leb-2 GFP-h* cotyledon leaves.

2.4. Endogenous Arabidopsis Aspartic proteinases analysis

Given our special interest in PSI A localization and trafficking routes and the alterations of ER morphology, an analysis of the endogenous Arabidopsis Aspartic proteinases genes was performed, with special focus on the PSI-containing ones – A1, A2 and A3. Importantly, all PSI-containing APs from Arabidopsis have a glycosylated PSI, contrary to PSI A, that is not glycosylated (Figure 4-A, red box). Next, the relative expression of the three APs was evaluated in WT plants by qPCR. It is possible to observe that AP1 and AP2 are more expressed in WT when compared to the AP3, whose expression is significantly decreased (Figure 4-B). However, looking at the expression of the same genes in the *leb-2 GFP-h* line, the AP3 was found to be upregulated, when compared to WT plants, presenting itself a three-fold expression increase (Figure 4-C).

Preprints (www.preprints.org) | NOT PEER-REVIEWED | Posted: 3 April 2023 doi:10.20944/preprints202304.0023.v1

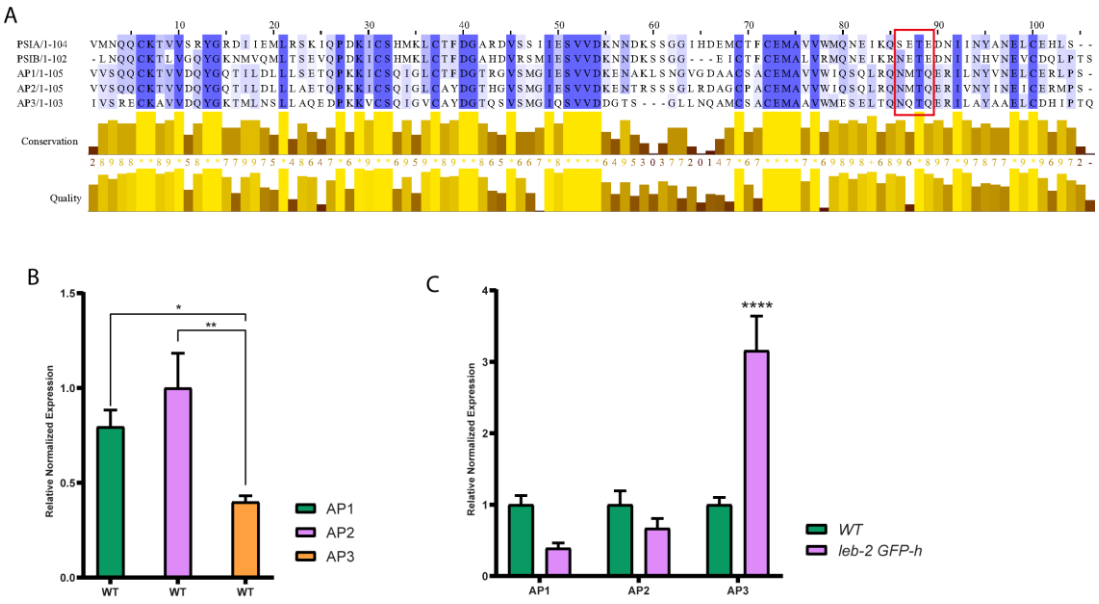

Figure 4 – *Arabidopsis thaliana* aspartic proteinases' expression in wild type and *leb-2 GFP-h*. (A) Alignment of cardosins' PSI A and B with Arabidopsis APs' PSIs (AP1, AP2 and AP3). Blue indicates percentage of similarity and the red box the glycosylation site. (B) Relative normalized expression of Arabidopsis APs in wild-type plants. (C) Relative normalized expression of Arabidopsis APs in the *leb-2 GFP-h* mutant, when compared to WT. Statistically experimental values are represented by: * (pvalue ≤0.05), ** (pvalue ≤0.01); ****(pvalue <0.0001).

2.5. Endomembrane genes expression testing

Given the alterations observed in the expression of Arabidopsis AP3 in the mutant background and given our interest in unravelling the intermediates in PSI A mediated sorting, the expression of some key-endomembrane trafficking genes was evaluated in the mutant background (Figure 5-A). Regarding the genes involved in protein trafficking to LV (*AtSYP52*) and PSV (*AtSYP51*), no significant alterations were registered in our analysis. *AtSYP22*, a SNARE involved in the vacuolar assembly also did not alter its expression. Its homologous *AtSYP23*, that does not have a transmembrane domain and its function is still unclear, was also analysed without significant alterations (Figure 5-B). Some SNAREs involved in vesicle docking and fusion were also tested. *AtSYP61* did not suffer any alterations in its expression, but *AtVAMP722* demonstrated upregulation in *leb-2 GFP-h*, when compared to WT. AtVAMP723, an ER-related homologue protein of the AtVAMP722, is the gene that demonstrates a higher significant overexpression. However, *AtVAMP721*, a Plasma Membrane related SNARE gene, did not alter its expression in the *leb-2 GFP-h* line (Figure 5-B).

Preprints (www.preprints.org) | NOT PEER-REVIEWED | Posted: 3 April 2023 doi:10.20944/preprints202304.0023.v1

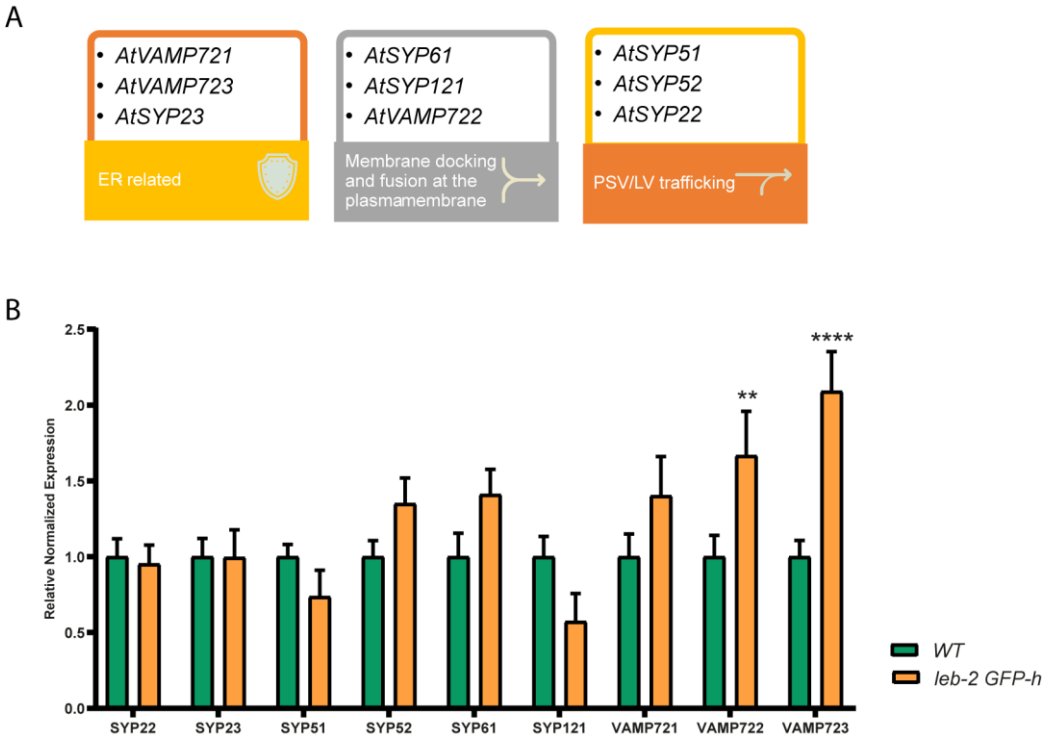

Figure 5 - Expression analysis by qRT-PCR of endomembrane-related genes in *leb-2 GFP-h* plants, when compared to WT plants. (A) Summary of the genes analysed and their relative role in endomembrane trafficking. (B) Bar graph showing the relative normalized expression of endomembrane genes in the mutant line. Only for *AtVAMP722* and *AtVAMP723* a significative alteration is observed. * Indicates statistically experimental values ($p < 0.05$), calculated using one-way ANOVA statistical tests.

3. Discussion

As sessile organisms, plants' fast and creative adaptation to the environment they are in is essential for their survival. The driving activities of the endomembrane system along with the individual dynamics of its organelles provide the plant cells with a unique plasticity to deal with a multitude of environmental cues. The secretory pathway, a major pathway of the endomembrane system, has its starting point in the Endoplasmic Reticulum (ER), a highly versatile network of continuous tubules and cisterns contacting with several organelles in the cell that coordinates with membrane compartments along the secretory and endocytic pathways [7–9]. Cardosin A and B PSIs are vacuolar sorting domains known for mediating the trafficking to the vacuole trough different pathways: PSI A mediates an unconventional Golgi-bypass, while PSI B mediates a conventional ER-Golgi route [39]. The direct ER-to-vacuole route has not been well described, despite more proteins have been described to follow this route. Recently a novel ER-derived compartment – ERMEC – has been implicated in chitinase A transport to the vacuole [42]. Also, in seeds, it has been described the direct ER-transport to the PSV dependent on ER-bodies. Nevertheless, the information available is fragmented and not all events of direct ER-to-vacuole transport seem to depend on the same mechanisms. Here, we aim at exploring the role of ER-bodies in ER export in WT and a mutant Arabidopsis line from a combined aspartic proteinases' and endomembrane perspective.

Preprints (www.preprints.org) | NOT PEER-REVIEWED | Posted: 3 April 2023 doi:10.20944/preprints202304.0023.v1

3.1. The leb-2 GFP-h Arabidopsis mutant

A search in the Nottingham Arabidopsis Stock Centre (NASC) database led us to the *leb-2 GFP-h* line, but little to no information on this mutant was provided, despite being described as similar to the *leb-1* mutant [40]. It is known that this mutated line has a single nucleotide change (CCT→TCT) in the first exon of PYK10/BGLU23 gene, which causes an amino acid substitution (P41S) on the PYK10/BGLU23 protein. Also, the PYK10/BGLU23 protein has been observed to accumulate in ER structures named ER bodies [40,43]. The mutated line showed a clear difference in size when compared to WT and the developmental assay performed evidenced clear differences. Such stages of the chronological progression of the plants' growth were defined based on the literature available [44] and the results obtained demonstrated that the *leb-2 GFP-h* mutation delayed its development at the appearance of the three rosette leaves and this delay was maintained from this point forward. To further understand and characterize the effects of the mutation in this Arabidopsis line, the ultrastructure of the cells from cotyledon leaves was assessed through TEM. In the *leb-2 GFP-h* line, we observed an intriguing structural anomaly in the ER. Although there is no published description for this line, there is another mutated line very similar to this, to which it is described the presence of significantly fewer and larger ER bodies than the wild-type line [40]. The structure we observed in the *leb-2 GFP-h* line could correspond to the long ER bodies observed by the team of Nagano [40] or, at least, these deformations in the ER could correspond to the ER bodies formation sites. Additionally, in our observations, enlarged Golgi cisternae and rounded Golgi bodies are visible, along with numerous vesicles in the cell's cytoplasm, which may be indicative of high metabolic activity in the cell. Since the mutated line presents a GFP-HDEL marker, we observed the ER morphology in the *leb-2 GFP-h* line. Our results revealed that this mutant possesses elongated structures at the ER, resembling the long ER bodies observed by Nagano et al. (2009) [40]. We also exposed the mutated plants to BFA, a fungal macrocyclic lactone that inhibits secretion and vacuolar protein transport in plant cells, as it blocks the recruitment of COPI coat proteins onto Golgi membranes, which leads to the direct fusion of most Golgi cisternae to the ER, ultimately ending in the formation of an ER-Golgi hybrid compartment [41]. In fact, the ER morphology of the *leb-2 GFP-h* line is affected by the BFA, as the ER bodies observed appear more rounded, so trafficking processes were affected as well.

3.2. PSIs-mediated sorting and unconventional routes

For the past years, several studies have been focused on cardosins along with their PSI domains, given the contributions of these domains in unveiling unconventional vacuolar sorting routes [26,39]. In fact, PSI A and PSI B are capable of directing proteins to the vacuole without matching any of the classic VSD types [26]. PSI A was demonstrated to mediate a route independent of the normal COPII vesicle machinery, in order to traffic between the ER and the Golgi, as it would still accumulate in the vacuole when co-expressed with the dominant negative mutant $SarI^{H74L}$ in *Nicotiana tabacum* leaves [39]. In the native organism (*Cynara cardunculus* - cardoon), cardosin A is mostly found in the PSVs of the stigmatic papillae [21,25]. However, when expressed in heterologous systems (*Arabidopsis thaliana* and *Nicotiana tabacum*), cardosin A's accumulation is observed in different types of vacuoles (PSV and LV) [25,26]. On the other hand, PSI B is secreted in cardoon flowers [39] and accumulates in vacuoles in heterologous systems [27,39]. Such characteristics highlight the advantageous use of these domains as reporters for the study of vacuolar trafficking and VSDs in plants.

In a process exclusive to plants, the ER bodies have been implicated as intermediate compartments in the transport of proteins destined to the PSV directly from the ER bypassing the Golgi [13]. Therefore, given what we know about the PSI A-mediated trafficking, it would be interesting to assess if these subcellular structures would

Preprints (www.preprints.org) | NOT PEER-REVIEWED | Posted: 3 April 2023 doi:10.20944/preprints202304.0023.v1

participate alongside PSI A and/or PSI B in this unconventional route. Our results revealed a vacuolar localization of the PSI A and B both in the Arabidopsis WT and mutant, consistent with what had been previously described [25–27], strengthening the view the cardoon PSIs as vacuolar sorting domains, as both were efficient in leading the mCherry tag to the vacuole and, therefore, seem to be not affected by the ER morphological defects. Moreover, in the *leb-2 GFP-h* line, no co-localization was observed with ER bodies, nor interference with PSI A or PSI B vacuolar sorting, indicating that probably this pathway is not used by the PSI A (Figure 6). On the contrary, preliminary results on PSI B overexpression in transgenic Arabidopsis cotyledons showed it to be accumulated in structures resembling ER bodies (Supplemental Figure 1-B), that were not observed for PSI A (Supplemental Figure 1-A). Being confirmed, these results open up new perspectives regarding the differences observed between the sorting processes mediated by the two PSIs, that partially rely on the glycosylation, present in PSI B but absent in PSI A [39]. Interestingly, from the 51 genes identified for APs in the Arabidopsis genome, only three contain the PSI domain [45] and an alignment of the PSI domains from those APs with PSI A and B revealed that all contain the glycosylation site present in PSI B (Figure 4-A, red box). Moreover, a search in the literature available, shows that most of the identified PSIs have the glycosylation site, and that this glycosylation site seems to be involved in the ER-to Golgi transport, elevating the PSI A unconventional characteristic to a more interesting level.

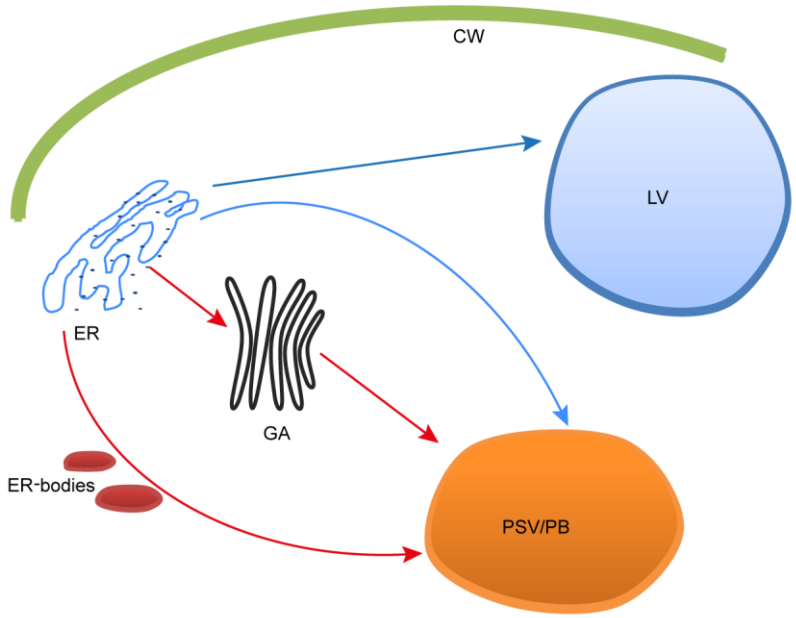

Figure 6 – Cardosins' PSIs routes observed in plants. PSI A is able to mediate an unconventional Golgi-bypass route to the LV, observed in *Nicotiana tabacum* leaves and Arabidopsis cotyledons (blue arrow). A putative route bypassing the Golgi to the PSV is predicted to exist in flowers and seeds (blue arrow, unconfirmed). The red arrows indicate putative routes mediated by PSI B.

Furthermore, the expression analysis of the three Arabidopsis APs also retrieved important information on the role of these proteinases. Chen and co-workers (2002)[46] used specific probes to analyze the expression of the three different genes and showed that AP A1 is detected in all tissues and is more abundant in leaves, while the other two genes are expressed either in flowers (A3) or in seeds (A2). Our results are in accordance with these observations, as AP3 expressions levels are significantly lower when compared to AP1 and AP2, which is not surprising since our study was conducted in Arabidopsis cotyledons and AP3 expression is mainly detected in flowers [46]. Surprisingly, when comparing the AP3 expression in the *leb-2 GFP-h* line with the wild type plants, we could verify a ~4-fold increase in the expression levels. Though intriguing, as AP3 is mainly expressed in flowers, this could indicate a putative connection between APs and the ER

Preprints (www.preprints.org) | NOT PEER-REVIEWED | Posted: 3 April 2023 doi:10.20944/preprints202304.0023.v1

bodies dependent route. Although little is known regarding the localization and function of AP3 in flowers, it has been described as a secreted protein in flower tissues. The parallel can be made with Cardosin B, a well-characterized AP from cardoon plants that was found to localize at the extracellular matrix [39]. Additionally, Nakano and his team [47] presented a thorough review on ER bodies and evidence that ER bodies can be involved in protein secretion, suggesting a role for these structures in the resistance against pathogens. It can be considered that both cardosin B and AP3 can be transported to the cell surface associated with ER bodies. Despite being a frail connection and lacking experimental evidence, it is worth to explore the trafficking of these proteins and their relationship with ER bodies in other physiological conditions and different organs.

3.3. Endomembrane system effectors expression level analysis

Given the alterations observed in the expression of Arabidopsis APs and cardosins' PSIs, it was decided to check the expression of several key-endomembrane system genes in the *leb-2 GFP-h* mutant, involved either in vacuolar sorting – AtSYP51/52 and AtSYP22 -, plasma membrane docking and fusion – AtSYP61, AtSYP121 and AtVAMP721/722 – or involved in ER vesicle fusion – AtVAMP723 and AtSYP23. Most of the genes tested do not show any significative variance in relation to the wild-type plants, indicating that the mutation does not interfere with most of the trafficking events, with special focus on the vacuolar trafficking. However, a significative upregulation was observed for AtVAMP722 and AtVAMP723, which is particularly evident for the last one. AtVAMP723 is a R-SNARE, involved in vesicle docking, fusion and budding, and its localization at the ER membranes [48] can be related to the formation and release of ER bodies, thus its expression being enhanced in the mutant background. On the other hand, the homologue AtVAMP722, shares the same roles, but in a diferent localization and it is known that it may be involved in the secretory trafficking to the plasma membrane [49]. Taking into account the results obtained for the AP3 expression in the mutant background and the hypothesis that its trafficking can be dependent on ER-bodies it is fair to assume an upregulation of a SNARE involved in trafficking to the cell membrane as is AtVAMP722. It would be interesting to explore in the future the relation between AtVAMP722 and ER-bodies, as, to our knowledge, no studies have been made conecting the two. Moreover, it has been reported that AtVAMP722 forms a complex with AtVAMP721 and SYP121 [50,51], that do not show any changes in our study. This points to an isolated role of AtVAMP722, or in complex with other unknown proteins, in this process. In fact, it has been reported that probably VAMP722 is the most relevant member of the VAMP72 family [52]. Despite the amount of information available on the mechanisms of membrane fusion and the intermediates in the process, there is still a lot of fragmented information and novel data being released that challenges the established view of the diferent processes, particularly when concerning the unconventional pathways.

4. Materials and Methods

4.1 Biological Material

From the Nottingham Arabidopsis Stock Center (NASC), one Arabidopsis thaliana line bearing defects in ER morphology was selected: N69081 (*leb-2 GFP-h*—unpublished). This line also harbours a GFP-HDEL marker that allows ER visualization. Seeds from the mutant line, as well as a wild-type (WT; col0) were sown and germinated in plates containing 2,2 g/L of Mourashige and Skooge medium (MS, Duchefa), with 1,5 % (w/v) sucrose, 0,7 % (w/v) Bacto-agar and pH 5.7. Plants were kept for 48 h at 4 °C and, following stratification, were grown at 22 °C with 60% humidity and 16 h light over 8 h dark photoperiod (OSRAM L 36 W/77 e OSRAM L 36 W/840) at the intensity of 110 μmol·m-2·s. After 12–15 days, seedlings were transferred to individual pots with fertilized substrate (SYRO PLANT) and grown under continuous light at 22 °C with 50–60% relative humidity and light intensity at 180 μmol·m-2·s.

Preprints (www.preprints.org) | NOT PEER-REVIEWED | Posted: 3 April 2023 doi:10.20944/preprints202304.0023.v1

The isolation and identification of leb-2 GFP-h mutant was performed by PCR from EMS-mutagenized GFP-h plants using the following primers: 5′ end gene-specific primer, 5′-TGTCAAGAGGTGCTCACAGAGGAAC, 3′ end gene-specific primer, 5′-CCAGCAAATGCAGATGGACCTGTAT. The PCR reactions were followed by a purification step using illustra™ GFX™ PCR DNA and Gel Band Purification Kit (cytiva, United States) and sent for sequencing. The PCR conditions for amplification of the genomic DNA were standard conditions, as described in the manufacturer's instructions (NZYTech, Portugal).

4.2 Transmission Electron Microscopy (TEM)

Small pieces of leaves from seedlings (12-15 days old) and mature plants of the *leb-2 GFP-h* mutant and wild-type, grown as described, were cut into pieces of approximately 1–2 mm for transmission electron microscopy. These were fixed in Na-PIPES (1.25% (w/v) and pH 7.2) with glutardialdehyde 2.5% (v/v) for 1 h at room temperature (RT). Then, the samples were washed with Na-PIPES 2.5% (w/v) (3 times for 10 min each) and post-fixated with a OsO4 4% (w/v) solution prepared in Na-PIPES 2.5% (w/v) pH 7.2, in a proportion of 1:1, for 1 h at RT. Post-fixation was followed by 3 washes with Na-PIPES 2.5 % (p/v) pH 7.2 for 10 min each. After these washes, proceeded the dehydration steps in an ethanol graded series at RT as follows: 10 % (v/v) for 10 minutes; 20 % (v/v), 30 % (v/v) and 50 % (v/v) for 15 minutes; and 70 % (v/v) and 100 % (v/v) for 20 minutes. The ethanol was then exchanged with propylene oxide for 20 min. The biological material was gradually infiltrated in increasing concentrations of EPON resin (Agar scientific): 10% (for 15 min) to 50% (overnight) and 100% (overnight). The samples were then transferred to oriented moulds, covered with resin, and polymerized at 60 °C overnight. Ultrathin sections (60–80 nm) were cut in UC6 Ultramicrotome (Leica, Carnaxide, Portugal) with a diamond knife (Diatome), placed in 400 mesh copper grids, post-stained with Uranyless EM Strain (Uranyless) and with Reynolds Lead citrate 3% (Uranyless) for 5 min each. After washing in distilled water to remove excess stain, grids were observed in a Jeol JEM 1400 Transmission Electron Microscope, and the images were acquired with an Orius DC200D camera (Gatan, Pleasanton, CA, USA). Image analysis and processing were done using ImageJ®/Fiji software.

4.3 Transient Transformation of Arabidopsis thaliana Seedlings through Vacuum Infiltration

For transient transformation of *A. thaliana*, the protocol established by Bernat-Silvestre et al. [53] was adapted. Seeds from the *leb-2 GFP-h* mutant and wild-type were sown and germinated in six-well plates and grown for 5 days, as previously described. For the transformation, Agrobacterium tumefaciens harboring the SP-PSIA–mCherry construct [26,39] were inoculated in LB medium with the appropriate antibiotics (kanamycin (50 μg/mL) and gentamicin (50 μg/mL)) and incubated for 24 h in agitation at 28 °C, until an OD600 of 2.2. Cultures were centrifuged for 15 min at 6000× g at room temperature, and the pellets were resuspended in infiltration buffer (liquid MS medium with 0.005% (v/v) Tween and 200 μM acetosyringone). This suspension remained at room temperature for 30–45 min, and then was poured onto the six-well plates with the Arabidopsis seedlings (4 mL per well); next, a vacuum was applied at 300 mbar for 1 min. The pressure was then slowly increased to 400 mbar, and a vacuum was applied for another minute. Finally, the bacterial suspension was fully removed, and the plates were covered with aluminum foil for 45 min to 1 h to improve agro-infection. After removing the aluminum foil, the plates were kept for 3 days under the previously mentioned growth conditions.

4.4 Transformation of Arabidopsis thaliana for stable expression

To generate transgenic PSIB plants, transformation was performed by the floral dip method [54]. SP-PSIB-mCherry construct that was previously available in the lab, was used for this purpose [26]. A small aliquot of Agrobacterium tumefaciens containing the clone was inoculated into 5 mL of LB (Luria Bertani) medium supplemented with the

Preprints (www.preprints.org) | NOT PEER-REVIEWED | Posted: 3 April 2023 doi:10.20944/preprints202304.0023.v1

appropriate antibiotics (kanamycin 50 µg/mL and gentamicin 20 µg/mL) and allowed to grow overnight (ON) at 28 °C, shaking. Then, the entire volume of the starter culture was inoculated in 250 mL of LB media supplemented with kanamycin and gentamicin at concentrations already described and stirred once more at 28 °C ON. The total volume was split into 50-mL Falcon tubes and centrifuged for 20 minutes at 5000 x g. The supernatant was discarded, and the pellet was resuspended in a 5 % (w/v) sucrose and 0.05 % (v/v) silwet solution. A. thaliana wild-type plants with a developed floral stem and flowers were used, from which the previously produced siliques were removed. Then, the plant's aerial portion was immersed in the Agrobacterium solution and gently shaken for 1 minute. This process was repeated three times with four different plants. Finally, the plants were returned to the greenhouse, and a plastic bag was wrapped around them to allow for moisture. The plants were left in these circumstances overnight before the bag was removed the next day. The flower stems were collected, dried, and the seeds they produced were collected when they showed well-developed siliques. The seeds from each initially transformed plant were stored separately and treated as different primary transformants. To select the transgenic plants, the antibiotic Hygromycin B (500 mg/mL; Duchefa Biochemie) was added, and the presence of the transgene was verified by PCR and Western blot (data not shown). Further research was conducted using the homozygous T3 transgenic lines.

4.5 Drug Treatment Assays

Brefeldin A (BFA) solution (50 µg/mL) was prepared in MS liquid medium, and 4 mL per well was poured over the infiltrated seedlings one day after the A. tumefaciens infiltration. A vacuum was applied as previously described. Seedlings were kept in the BFA solution for about 16–18 h before the cells were imaged.

4.6 CLSM Analysis

Arabidopsis seedlings were observed and analyzed using a confocal laser scanning microscope (CLSM, Leica STELLARIS 8). Cotyledons from Arabidopsis seedlings were prepared by placing the biological material on a slide with a drop of sterile water covered by a cover slip. In all situations, the abaxial epidermis was observed. For mCherry, using 561 nm excitation, emissions were detected between 580 and 630 nm. In the case of GFP, the excitation wavelength used was 488 nm, and the emissions were detected between 500 and 528 nm. Analysis and quantification of the acquired images were performed using the ImageJ®/Fiji software.

4.7 cDNA Preparation

Total RNA was prepared using the "NZY Total RNA Isolation Kit" (NZYTech, Lisboa, Portugal) by following the manufacturer guidelines and starting from 100 mg of seedling tissue. Three biological replicates were prepared, and the respective samples were quantified using a DS-11 microvolume Spectrophotometer (DeNovix, Wilmington, NC, USA). The RNAs were stored at -80 °C. To produce the cDNA from the isolated RNA, NZY First-Strand cDNA Synthesis kit (NZYTech, Lisboa, Portugal) was used according to the manufacturer's instructions. The cDNA solution was stored at -20 °C.

4.8 Gene Selection

The genes selected for quantitative RT-PCR in this study were chosen based on their on their product localization, role, interaction partners, and literature references (Table 1), as it had been previously investigated [41].

Preprints (www.preprints.org) | NOT PEER-REVIEWED | Posted: 3 April 2023 doi:10.20944/preprints202304.0023.v1

Table 1 – Genes selected for qPCR analysis, and their respective role and localization.

Genes	Identifier	Role and Localisation	Ref.
AtSAND-1	AT2G28390	Housekeeping gene.	[55,56]
AtGAPDH	AT1G13440	Housekeeping gene.	[55,56]
AtUBC9	AT4G27960	Housekeeping gene.	[55,56]
AtSYP51	AT1G16240.1	Transport to the PSV, vesicle docking and fusion. Enables SNAP receptor activity, SNARE binding and protein binding. Interacts with VTI12.	[56,57]
AtSYP121	AT3G11820.1	Syntaxin found in the plasma membrane. Capable of forming a complex with SYP51 and VTI11.	[58,59]
AtSYP23	AT4G17730.2	Transmembrane domain-free cytosolic syntaxin. Role in transport vesicles docking or fusion with the prevacuolar membrane, enabling SNAP receptor activity and SNARE binding.	[56,60]
AtVAMP723	AT2G33110.1	Found in the endoplasmic reticulum. Directs transport vesicles towards their intended membrane and/or fusing them there.	[48]
AtSYP22	AT5G46860.1	Syntaxin-related protein necessary for vacuolar assembly. Localized in the vacuolar membranes, late endosome and trans-Golgi network (TGN) transport vesicles.	[56,60]
AtVAMP722	AT2G33120.2	Directs transport vesicles towards their intended membrane and/or fusing them there. Response to biotic stress. Outlines a complex that includes SYP121.	[61,62]
AtVAMP721	AT1G04750	Involved in TGN/early endosome mediated secretory trafficking to the plasma membrane, contributing to cell plate formation.	[48,49]
AtSYP61	AT1G28490.1	Vesicle trafficking protein. Along with SYP121, coordinates plasma membrane aquaporin PIP2;7 trafficking to modulate membrane water permeability. Complexes with VTI12.	[56,58]
AtSYP52	AT1G79590.2	Localized to TGN/vacuole, participates in the route to the Lytic vacuole and complexes with VTI11.	[56,57]
AtAP1	AT1G11910	Saposin-like aspartyl protease with a PSI domain, located along the secretory pathway.	[56]
AtAP2	AT1G62290	Saposin-like aspartyl protease with a PSI domain, located in the vacuole and secretory vesicles.	[56]
AtAP3	AT4G04460	Saposin-like aspartyl protease with a PSI domain, secreted to the extracellular region.	[56]

4.9 Quantitative RT-PCR

All the primers used in this work were already available in the laboratory, with all of their reactions optimized[63,64]. The plate design was created using the software Bio-Rad CFX Maestro 1.0 (BioRad, Hercules, CA, USA). The qPCR reaction had a final volume of

Preprints (www.preprints.org) | NOT PEER-REVIEWED | Posted: 3 April 2023 doi:10.20944/preprints202304.0023.v1

10 µL where 2 µL were cDNA and 8 µL were a master mix composed by: NZYSupreme qPCR Green Master Mix (2x) (NZYTech, Lisboa, Portugal), 400 nM of each primer (forward and reverse – Table 2) and water. The protocol used the following amplification conditions: initial denaturation (95 °C for 3 min); 40 cycles of amplification and quantification (95 °C for 10 s,56 °C for 10 s and 72 °C for 30 s, with a single fluorescent measurement) and melting curve generation (65 °C to 95 °C, with one fluorescence read every 0.5 °C). The equipment used was CFX96 Real-Time System (BioRad, Hercules, CA, USA). Using Bio-Rad CFX Maestro (version 1.0) software, the cycle threshold (Ct) and expression tests were calculated by comparing them with wild type.

Table 2 – Primers used in the qPCR assay.

Genes	Primer Forward	Primer Reverse
SAND[1]	AACTCTATGCAGCATTTGATCCACT	TGATTGCATATCTTTATCGCCATC
GAPDH[1]	TTGGTGACAACAGGTCCAAGCA	AAACTTGTCGCTCAATGCAATC
UBC9[1]	TCACAATTTCCAAGGTGCTGC	TCATCTGGGTTTGGATCCGT
SYP51	TGGCGTCTTCATCGGATTCATGG	AGCTGAAGCACGACGCTGAGCA
SYP121	TCCTCCGATCGAACCAGGACCTC	TTCTCGCCGGTGACGGTGAA
SYP23	GCAGCGTGCCCTTCTTGTGG	TCCTTGGGCAGTTGCAGCGTA
VAMP723	CCCGTGGTGTGATATGTGAG	CCACAAACCGAGAGGATGAT
SYP22	CGAGGAAATTCAATGGTGGT	ACGTGGAGACTCCGGTATTG
VAMP722	CAATTTGTGGGGGATTCAAC	GATCTTGGGAAGCACAGAGC
SYP61	TTGAAAAACGGAGGAGATGG	TTCACTTGCATGACCTGCTC
SYP52	ATGTGGTGGCAACTTGTGAA	CTTTGCCTCACAGACACGAA
AtAP1	GGCATTGAGTCGGTGGTGGACA	TCTCACATGCAGAACACGCAGCA
AtAP2	GGGGATTGAATCGGTGGTGGA	ACATGCAGGACAACCCGCGTCT
AtAP3	TGCAAGGCCGTGGTGGATCA	GCGCAGACTCCAATTTGTGAGCA

Author Contributions: Conceptualisation and methodology, A.S., M.S., S.P., J.P. and C.P.; investigation, T.C., S.O. I.M., J.N. and M.S.; formal analysis and software, T.C., J.N., M.S., A.S. and C.P.; project administration and funding acquisition, C.P. and J.P.; writing—original draft, T.C., J.N., M.S., S.O., I.M. and C.P.; writing—review and editing, S.P, C.P. and J.P.; supervision, A.S., S.P., J.P. and C.P. All authors have read and agreed to the published version of the manuscript.

Funding: This research was funded by the Portuguese Foundation for Science and Technology (FCT) and also supported by national funds through FCT, within the scope of UIDB/05748/2020 and UIDP/05748/2020. Miguel Sampaio is the recipient of a PhD fellowship funded by the Portuguese Foundation for Science and Technology (FCT) (SFRH/UIDB/151042/2021).

Data Availability Statement: Not applicable

Conflicts of Interest: The authors declare no conflict of interest.

Preprints (www.preprints.org) | NOT PEER-REVIEWED | Posted: 3 April 2023 doi:10.20944/preprints202304.0023.v1

Supplementary material:

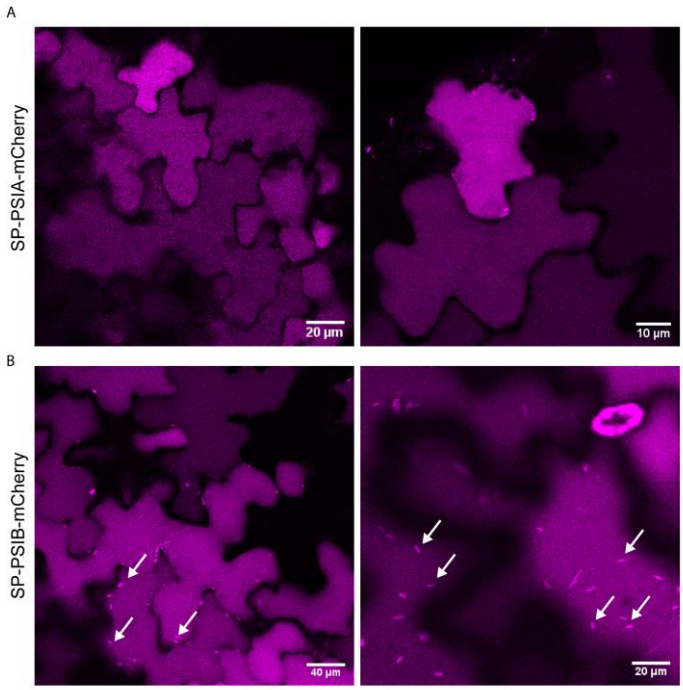

Supplemental Figure 1 – Subcellular localization of SP-PSIA/B-mCherry in cotyledon leaves of Arabidopsis transgenic plants overexpressing SP-PSIA/B-mCherry, respectivelly. (A) SP-PSIA-mCherry is detected inside vacuoles of cotyledon cells. (B) SP-PSI-mCherry is observed inside the vacuole of cotyledon cells and also in elongated structures in sytoplasm resembling ER-bodies (arrows).

References

1. Morita, M.T.; Shimada, T. The Plant Endomembrane System—A Complex Network Supporting Plant Development and Physiology. *Plant Cell Physiol.* **2014**, *55*, 667–671, doi:10.1093/pcp/pcu049.

2. Cevher-Keskin, B. Endomembrane Trafficking in Plants. *Electrodialysis* **2020**, 1–22, doi:10.5772/intechopen.91642.

3. Frigerio, L.; Hawes, C. The endomembrane system: A green perspective. *Traffic* **2008**, *9*, 1563, doi:10.1111/J.1600-0854.2008.00795.X.

4. Stefano, G.; Hawes, C.; Brandizzi, F. ER - the key to the highway. *Curr. Opin. Plant Biol.* **2014**, *22*, 30–38, doi:10.1016/j.pbi.2014.09.001.

5. Wang, X.; Chung, K.P.; Lin, W.; Jiang, L. Protein secretion in plants: Conventional and unconventional pathways and new techniques. *J. Exp. Bot.* **2018**, *69*, 21–37, doi:10.1093/jxb/erx262.

6. Wang, X.; Xu, M.; Gao, C.; Zeng, Y.; Cui, Y.; Shen, W.; Jiang, L. The roles of endomembrane trafficking in plant abiotic stress responses. *J. Integr. Plant Biol.* **2020**, *62*, 55–69, doi:10.1111/jipb.12895.

7. Staehelin, L.A. The plant ER: a dynamic organelle composed of a large number of discrete functional domains. *Plant J.* **1997**, *11*, 1151–1165, doi:10.1046/j.1365-313X.1997.11061151.x.

8. Stefan, C.J.; Manford, A.G.; Emr, S.D. ER-PM connections: Sites of information transfer and inter-organelle communication. *Curr. Opin. Cell Biol.* **2013**, *25*, 434–442, doi:10.1016/j.ceb.2013.02.020.

9. Stefano, G.; Renna, L.; Lai, Y.; Slabaugh, E.; Mannino, N.; Buono, R.A.; Otegui, M.S.; Brandizzi, F. ER network homeostasis is critical for plant endosome streaming and endocytosis. *Cell Discov.* **2015**, *1*, 15033, doi:10.1038/celldisc.2015.33.

10. Nakano, R.T.; Matsushima, R.; Ueda, H.; Tamura, K.; Shimada, T.; Li, L.; Hayashi, Y.; Kondo, M.; Nishimura, M.; Hara-Nishimura, I. GNOM-LIKE1/ERMO1 and SEC24a/ERMO2 Are Required for Maintenance of Endoplasmic Reticulum Morphology in Arabidopsis thaliana . *Plant Cell* **2009**, *21*, 3672–3685, doi:10.1105/tpc.109.068270.

11. Quader, H.; Schnepf, E. Endoplasmic reticulum and cytoplasmic streaming: Fluorescence microscopical observations in adaxial epidermis cells of onion bulb scales. *Protoplasma* **1986**, *131*, 250–252, doi:10.1007/BF01282989.

12. Matsushima, R.; Hayashi, Y.; Yamada, K.; Shimada, T.; Nishimura, M.; Hara-Nishimura, I. The ER Body, a Novel Endoplasmic Reticulum-Derived Structure in Arabidopsis. *Plant Cell Physiol.* **2003**, *44*, 661–666, doi:10.1093/pcp/pcg089.

13. Hara-Nishimura, I.; Matsushima, R.; Shimada, T.; Nishimura, M. Diversity and Formation of Endoplasmic Reticulum-Derived Compartments in Plants. Are These Compartments Specific to Plant Cells? *Plant Physiol.* **2004**, *136*, 3435–3439, doi:10.1104/pp.104.053876.

14. Sampaio, M.; Neves, J.; Cardoso, T.; Pissarra, J.; Pereira, S.; Pereira, C. Coping with Abiotic Stress in Plants—An Endomembrane Trafficking Perspective. *Plants* **2022**, *11*, 1–15, doi:https://www.mdpi.com/2223-7747/11/3/338.

15. Marcos Lousa, C.; Gershlick, D.C.; Denecke, J. Mechanisms and Concepts Paving the Way towards a Complete Transport Cycle of Plant Vacuolar Sorting Receptors. *Plant Cell* **2012**, *24*, 1714–1732, doi:10.1105/tpc.112.095679.

16. Rojo, E.; Denecke, J. What is moving in the secretory pathway of plants? *Plant Physiol.* **2008**, *147*, 1493–503, doi:10.1104/pp.108.124552.

17. Olbrich, A.; Hillmer, S.; Hinz, G.; Oliviusson, P.; Robinson, D.G. Newly formed vacuoles in root meristems of barley and pea seedlings have characteristics of both protein storage and lytic vacuoles. *Plant Physiol.* **2007**, *145*, 1383–1394, doi:10.1104/pp.107.108985.

18. Paris, N.; Stanley, C.M.; Jones, R.L.; Rogers, J.C. Plant Cells Contain Two Functionally Distinct Vacuolar Compartments. *Cell* **1996**, *85*, 563–572, doi:10.1016/S0092-8674(00)81256-8.

19. Ramalho-Santos, M.; Verissimo, P.; Cortes, L.; Samyn, B.; Van Beeumen, J.; Pires, E.; Faro, C. Identification and proteolytic processing of procardosin A. *Eur. J. Biochem.* **1998**, *255*, 133–138, doi:10.1046/j.1432-1327.1998.2550133.x.

20. Vieira, M.; Pissarra, J.; Veríssimo, P.; Castanheira, P.; Costa, Y.; Pires, E.; Faro, C. Molecular cloning and characterization of cDNA encoding cardosin B, an aspartic proteinase accumulating extracellularly in the transmitting tissue of Cynara cardunculus L. *Plant Mol. Biol.* **2001**, *45*, 529–39.

21. Ramalho-Santos, M.; Pissarra, J.; Veríssimo, P.; Pereira, S.; Salema, R.; Pires, E.; Faro, C.J. Cardosin A, an abundant aspartic proteinase, accumulates in protein storage vacuoles in the stigmatic papillae of Cynara cardunculus L. *Planta* **1997**, *203*, doi:10.1007/s004250050183.

22. Pissarra, J.; Pereira, C.; Soares, D.; Figueiredo, R.; Duarte, P.; Teixeira, J.; Pereira, S. From Flower to Seed Germination in Cynara cardunculus : A Role for Aspartic Proteinases. *Int. J. Plant Dev. Biol.* **2007**, *1*, 274–281.

23. Pereira, C.S.; da Costa, D.S.; Pereira, S.; de Moura Nogueira, F.; Albuquerque, P.M.; Teixeira, J.; Faro, C.; Pissarra, J. Cardosins in postembryonic development of cardoon: towards an elucidation of the biological function of plant aspartic proteinases. *Protoplasma* **2008**, *232*, 203–213, doi:10.1007/s00709-008-0288-9.

24. Oliveira, A.; Pereira, C.; Costa, D.S. d. D.S. da; Teixeira, J.; Fidalgo, F.; Pereira, S.; Pissarra, J. Characterization of aspartic proteinases in C. cardunculus L. callus tissue for its prospective transformation. *Plant Sci.* **2010**, *178*, 140–146, doi:10.1016/j.plantsci.2009.11.008.

25. Duarte, P.; Pissarra, J.; Moore, I. Processing and trafficking of a single isoform of the aspartic proteinase cardosin A on the vacuolar pathway. *Planta* **2008**, *227*, 1255–1268, doi:10.1007/s00425-008-0697-1.

26. Pereira, C.; Pereira, S.; Satiat-Jeunemaitre, B.; Pissarra, J. Cardosin A contains two vacuolar sorting signals using different vacuolar routes in tobacco epidermal cells. *Plant J.* **2013**, n/a-n/a, doi:10.1111/tpj.12274.

27. da Costa, D.S.; Pereira, S.; Moore, I.; Pissarra, J. Dissecting cardosin B trafficking pathways in heterologous systems. *Planta* **2010**, *232*, 1517–1530, doi:10.1007/s00425-010-1276-9.

28. Simões, I.; Faro, C. Structure and function of plant aspartic proteinases. *Eur. J. Biochem.* **2004**, *271*, 2067–75, doi:10.1111/j.1432-1033.2004.04136.x.

29. Soares, A.; Ribeiro Carlton, S.M.; Simões, I. Atypical and nucellin-like aspartic proteases: emerging players in plant developmental processes and stress responses. *J. Exp. Bot.* **2019**, *70*, 2059–2076, doi:10.1093/jxb/erz034.

30. Egas, C.; Lavoura, N.; Resende, R.; Brito, R.M.M.; Pires, E.; de Lima, M.C.P.; Faro, C. The Saposin-like Domain of the Plant Aspartic Proteinase Precursor Is a Potent Inducer of Vesicle Leakage. *J. Biol. Chem.* **2002**, *275*, 38190–38196, doi:10.1074/jbc.m006093200.

31. Terauchi, K.; Asakura, T.; Ueda, H.; Tamura, T.; Tamura, K.; Matsumoto, I.; Misaka, T.; Hara-Nishimura, I.; Abe, K. Plant-specific insertions in the soybean aspartic proteinases, soyAP1 and soyAP2, perform different functions of vacuolar targeting. *J. Plant Physiol.* **2006**, *163*, 856–62, doi:10.1016/j.jplph.2005.08.007.

32. De Moura, D.C.; Bryksa, B.C.; Yada, R.Y. In silico insights into protein-protein interactions and folding dynamics of the saposin-like domain of Solanum tuberosum aspartic protease. *PLoS One* **2014**, *9*, 18–22, doi:10.1371/journal.pone.0104315.

33. Frey, M.E.; D'Ippolito, S.; Pepe, A.; Daleo, G.R.; Guevara, M.G. Transgenic expression of plant-specific insert of potato aspartic proteases (StAP-PSI) confers enhanced resistance to Botrytis cinerea in Arabidopsis thaliana. *Phytochemistry* **2018**, *149*, 1–11, doi:10.1016/j.phytochem.2018.02.004.

34. Muñoz, F.; Palomares-Jerez, M.F.; Daleo, G.; Villalaín, J.; Guevara, M.G. Possible mechanism of structural transformations induced by StAsp-PSI in lipid membranes. *Biochim. Biophys. Acta - Biomembr.* **2014**, *1838*, 339–347, doi:10.1016/j.bbamem.2013.08.004.

35. De Caroli, M.; Lenucci, M.S.; Di Sansebastiano, G.-P.; Dalessandro, G.; De Lorenzo, G.; Piro, G. Protein trafficking to the cell wall occurs through mechanisms distinguishable from default sorting in tobacco. *Plant J.* **2011**, *65*, 295–308, doi:10.1111/j.1365-313X.2010.04421.x.

36. De Marchis, F.; Bellucci, M.; Pompa, A. Unconventional pathways of secretory plant proteins from the endoplasmic reticulum to the vacuole bypassing the Golgi complex. *Plant Signal. Behav.* **2013**, *8*, doi:10.4161/psb.25129.

37. Stigliano, E.; Faraco, M.; Neuhaus, J.-M.M.; Montefusco, A.; Dalessandro, G.; Piro, G.; Di Sansebastiano, G.-P. Pietro Two glycosylated vacuolar GFPs are new markers for ER-to-vacuole sorting. *Plant Physiol. Biochem.* **2013**, *73*, 337–343, doi:10.1016/j.plaphy.2013.10.010.

38. Sansebastiano, G.P. Di; Barozzi, F.; Piro, G.; Denecke, J.; Lousa, C.D.M. Trafficking routes to the plant vacuole: Connecting alternative and classical pathways. *J. Exp. Bot.* **2018**, *69*, 79–90, doi:10.1093/jxb/erx376.

39. Vieira, V.; Peixoto, B.; Costa, M.; Pereira, S.; Pissarra, J.; Pereira, C. N-linked glycosylation modulates Golgi-independent vacuolar sorting mediated by the plant specific insert. *Plants* **2019**, *8*, 1–21, doi:10.3390/plants8090312.

40. Nagano, A.J.; Maekawa, A.; Nakano, R.T.; Miyahara, M.; Higaki, T.; Kutsuna, N.; Hasezawa, S.; Hara-Nishimura, I. Quantitative analysis of ER body morphology in an arabidopsis mutant. *Plant Cell Physiol.* **2009**, *50*, 2015–2022, doi:10.1093/pcp/pcp157.

41. Nebenführ, A.; Ritzenthaler, C.; Robinson, D.G. Brefeldin A: Deciphering an enigmatic inhibitor of secretion. *Plant Physiol.* **2002**, *130*, 1102–1108, doi:10.1104/pp.011569.

42. De Caroli, M.; Barozzi, F.; Renna, L.; Piro, G.; Di Sansebastiano, G. Pietro Actin and microtubules differently contribute to vacuolar targeting specificity during the export from the er. *Membranes (Basel).* **2021**, *11*, doi:10.3390/membranes11040299.

43. Matsushima, R.; Kondo, M.; Nishimura, M.; Hara-Nishimura, I. A novel ER-derived compartment, the ER body, selectively

accumulates a β-glucosidase with an ER-retention signal in Arabidopsis. *Plant J.* **2003**, *33*, 493–502, doi:10.1046/J.1365-313X.2003.01636.X.

44. Boyes, D.C.; Zayed, A.M.; Ascenzi, R.; McCaskill, A.J.; Hoffman, N.E.; Davis, K.R.; Görlach, J. Growth Stage–Based Phenotypic Analysis of Arabidopsis: A Model for High Throughput Functional Genomics in Plants. *Plant Cell* **2001**, *13*, 1499–1510, doi:10.1105/TPC.010011.

45. Faro, C.; Gal, S. Aspartic Proteinase Content of the Arabidopsis Genome. *Curr. Protein Pept. Sci.* **2005**, *6*, 493–500, doi:10.2174/138920305774933268.

46. Chen, X.; Pfeil, J.E.; Gal, S. The three typical aspartic proteinase genes of Arabidopsis thaliana are differentially expressed. *Eur. J. Biochem.* **2002**, *269*, 4675–4684, doi:10.1046/j.1432-1033.2002.03168.x.

47. Ito, Y.; Uemura, T.; Nakano, A. *Formation and maintenance of the golgi apparatus in plant cells*; 1st ed.; Elsevier Inc., 2014; Vol. 310; ISBN 9780128001806.

48. Zhang, B.; Karnik, R.; Wang, Y.; Wallmeroth, N.; Blatt, M.R.; Grefen, C. The arabidopsis R-SNARE VAMP721 interacts with KAT1 and KC1 K+ channels to moderate K+ current at the plasma membrane. *Plant Cell* **2015**, *27*, 1697–1717, doi:10.1105/tpc.15.00305.

49. Zhang, L.; Zhang, H.; Liu, P.; Hao, H.; Jin, J.B.; Lin, J. Arabidopsis R-SNARE Proteins VAMP721 and VAMP722 Are Required for Cell Plate Formation. *PLoS One* **2011**, *6*, e26129, doi:10.1371/JOURNAL.PONE.0026129.

50. Laloux, T.; Matyjaszczyk, I.; Beaudelot, S.; Hachez, C.; Chaumont, F. Interaction Between the SNARE SYP121 and the Plasma Membrane Aquaporin PIP2;7 Involves Different Protein Domains. *Front. Plant Sci.* **2021**, *11*, 1–17, doi:10.3389/fpls.2020.631643.

51. Hachez, C.; Laloux, T.; Reinhardt, H.; Cavez, D.; Degand, H.; Grefen, C.; De Rycke, R.; Inzé, D.; Blatt, M.R.; Russinova, E.; et al. Arabidopsis SNAREs SYP61 and SYP121 coordinate the trafficking of plasma membrane aquaporin PIP2;7 to modulate the cell membrane water permeability. *Plant Cell* **2014**, *26*, 3132–3147, doi:10.1105/tpc.114.127159.

52. Bassham, D.C.; Blatt, M.R. SNAREs: cogs and coordinators in signaling and development. *Plant Physiol.* **2008**, *147*, 1504–1515, doi:10.1104/pp.108.121129.

53. Bernat-Silvestre, C.; De Sousa Vieira, V.; Sánchez-Simarro, J.; Aniento, F.; Marcote, M.J. Transient Transformation of A. thaliana Seedlings by Vacuum Infiltration BT - Arabidopsis Protocols. In *Methods in Molecular Biology*; Sanchez-Serrano, J.J., Salinas, J., Eds.; Springer US: New York, NY, 2021; Vol. 2200, pp. 147–155 ISBN 978-1-0716-0880-7.

54. Clough, S.J.; Bent, A.F. Floral dip: A simplified method for Agrobacterium-mediated transformation of Arabidopsis thaliana. *Plant J.* **1998**, *16*, 735–743, doi:10.1046/j.1365-313X.1998.00343.x.

55. Czechowski, T.; Stitt, M.; Altmann, T.; Udvardi, M.K.; Scheible, W.R. Genome-wide identification and testing of superior reference genes for transcript normalization in arabidopsis. *Plant Physiol.* 2005, *139*, 5–17.

56. TAIR - Home Page.

57. De Benedictis, M.; Bleve, G.; Faraco, M.; Stigliano, E.; Grieco, F.; Piro, G.; Dalessandro, G.; Di Sansebastiano, G. Pietro AtSYP51/52 functions diverge in the post-golgi traffic and differently affect vacuolar sorting. *Mol. Plant* **2013**, *6*, 916–930,

doi:10.1093/mp/sss117.

58. Hachez, C.; Laloux, T.; Reinhardt, H.; Cavez, D.; Degand, H.; Grefen, C.; De Rycke, R.; Inzé, D.; Blatt, M.R.; Russinova, E.; et al. Arabidopsis SNAREs SYP61 and SYP121 coordinate the trafficking of plasma membrane aquaporin PIP2;7 to modulate the cell membrane water permeability. *Plant Cell* **2014**, *26*, 3132–3147, doi:10.1105/tpc.114.127159.

59. Eisenach, C.; Chen, Z.H.; Grefen, C.; Blatt, M.R. The trafficking protein SYP121 of Arabidopsis connects programmed stomatal closure and K+ channel activity with vegetative growth. *Plant J.* **2012**, *69*, 241–251, doi:10.1111/j.1365-313X.2011.04786.x.

60. Shirakawa, M.; Ueda, H.; Shimada, T.; Koumoto, Y.; Shimada, T.L.; Kondo, M.; Takahashi, T.; Okuyama, Y.; Nishimura, M.; Hara-Nishimura, I. Arabidopsis Qa-SNARE SYP2 proteins localized to different subcellular regions function redundantly in vacuolar protein sorting and plant development. *Plant J.* **2010**, *64*, 924–935, doi:10.1111/j.1365-313X.2010.04394.x.

61. Kwon, C.; Bednarek, P.; Schulze-Lefert, P. Secretory pathways in plant immune responses. *Plant Physiol.* **2008**, *147*, 1575–1583, doi:10.1104/pp.108.121566.

62. Kwon, C.; Neu, C.; Pajonk, S.; Yun, H.S.; Lipka, U.; Humphry, M.; Bau, S.; Straus, M.; Kwaaitaal, M.; Rampelt, H.; et al. Co-option of a default secretory pathway for plant immune responses. *Nature* **2008**, *451*, 835–840, doi:10.1038/nature06545.

63. Neves, J.; Sampaio, M.; Séneca, A.; Pereira, S.; Pissarra, J.; Pereira, C. Abiotic Stress Triggers the Expression of Genes Involved in Protein Storage Vacuole and Exocyst-Mediated Routes. *Int. J. Mol. Sci.* **2021**, *22*, doi:https://doi.org/10.3390/ijms221910644.

64. Neves, J.; Monteiro, J.; Sousa, B.; Soares, C.; Pereira, S.; Fidalgo, F.; Pissarra, J.; Pereira, C. Relevance of the Exocyst in Arabidopsis exo70e2 Mutant for Cellular Homeostasis under Stress. *Int. J. Mol. Sci. 2023, Vol. 24, Page 424* **2022**, *24*, 424, doi:10.3390/IJMS24010424.